(2)

Technical Report 1406
March 1991

Battle Group Alternative Communications

A Study of the SHF Non-Satellite Communications Channel

J. W. Rockway
R. R. James

4

NAVAL OCEAN SYSTEMS CENTER

San Diego, California 92152–5000

J. D. FONTANA, CAPT, USN
Commander

H. R. TALKINGTON, Acting
Technical Director

ADMINISTRATIVE INFORMATION

The work described here was performed by the Electro-Optic Systems Branch, Code 844, Naval Ocean Systems Center, for the Office of Naval Technology. The work was sponsored by the Office of Naval Technology under Program Element 0602232N, Project R3211, and Accession Number DN300067.

Released by
R. P. Schindler, Head
Electro-Optic Systems
Branch

Under authority of
Dr. M. S. Kvigne, Head
Satellite Communications
Division

SB

SUMMARY

OBJECTIVE

Evaluate the value of the SHF (3-30 GHz) band as a non-satellite Navy Battle Group (NBG) communication link. Both line-of-sight and over-the-horizon communication channels are evaluated.

RESULTS

Considerable data were generated concerning the examination of three frequencies spanning the SHF band. Analysis indicates that the NBG communication link can support megabit signaling rates for many communication range and evaporation duct height configurations.

RECOMMENDATIONS

A program should be started to consider the value of a system based on the NBG communication link. Efforts should include system engineering, RF engineerring, network engineering, and experimental evaluation.

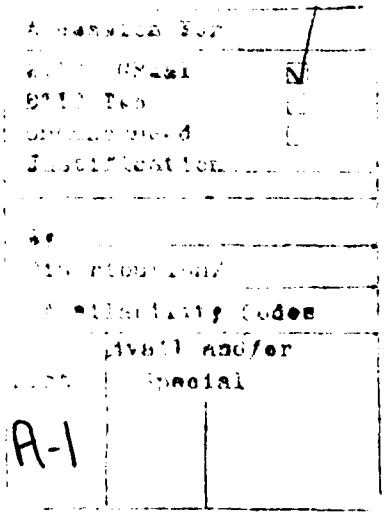

CONTENTS

FIGURES

TABLES

1.0 INTRODUCTION

This effort supports the alternative communications media task of the Naval Ocean Systems Center Navy Exploratory Development Block Program. The specific objective is to evaluate the value of the super high frequency (SHF) band (3-30 GHz) as a non-satellite Navy Battle Group (NBG) communication link. Both line-of-sight and over-the-horizon communication channels are evaluated.

Section 2 presents the background of this effort. Section 3 describes the system by including a discussion of the transmitter, receiver, and modem. Section 4 discusses the propagation channel which includes both line-of-sight and over-the-horizon propagation. The over-the-horizon discussion considers the effects of diffraction, ducting, and scattering. This section also discusses fading and attenuation due to atmosphere and rain. Section 5 presents an analytical approach for evaluating the SHF non-satellite channel and is used to evaluate non-satellite SHF NBG communications link performance. Section 6 concludes with a summary and a list of recommendations.

2.0 BACKGROUND

While lack of channel or bandwidth availability is the most frequently expressed communications problem in Navy Battle Group (NBG) communicatons, the actual issue is probably communications volatility (Clapp, 1988). NBG communciations is very transitory. There is no instantaneous guarantee of the quantity, quality, or timeliness of available communications.

The transitory nature of NBG communications is due to stress on the NBG communications system. Stress can originate either internally or externally. Changing requirements arise from the various user communities and can be classified as internal stress. Sources of internal stress can include mission changes, traffic loading, emission control, and security constraints. The changing environment results in stress sources external to the users. Sources of external stress can include equipment reliability, propagation changes, interference, and hostile jamming. Any combination of internal and external stress can appear in any given situation. These stresses are not isolated. These stresses result in orders of magnitude changes in quality, quantity, and timeliness.

The Navy currently uses the following techniques to mitigate internal and external stresses: traffic prioritization, communication planning, and link reallocation. These procedures do not address the large dynamic variations in NBG communication quality, quantity, and timeliness.

The primary technical focus is on the use of spread spectrum technology to improve NBG communications under stress. Major programs are focused on improving performance during jamming and other interference. However, some shortcomings of spread spectrum techniques are now becoming evident. The shortcomings include anti-jam (AJ) margins (endurance for an improving threat capability), electromagnetic compatability (EMC) problems, loss of capacity, cost, and interface difficulties with user systems.

Recent technical efforts consider network technology. The Navy Communication Support System (CSS) and the Navy Exploratory Development Block Program in communications have made networking their primary focus (Clapp, 1988). Networking appears to provide a means of achieving acceptable NBG communications in a stressed situation. Networking is especially useful for the routing of data around links and nodes that are congested or inoperative. The usefulness of networking for a communication system under stress is a function of the number of alternative communication capabilities available. Basic networking enhances the importance of new media and techniques to the NBG communication system. Any new communications media and technique can be incorporated into the NBG communication system through standardized interfaces and consequently shared by the user community. These new capabilities will provide flexibility through networking for the NBG communication system to respond to internal and external stress.

Several potential communication channels not currently exploited by the Navy include ducting, radio frequency (RF) and optical troposcatter, and remotely piloted vehicle (RPV) communication relays. This effort considers only troposcatter and ducting in the SHF band.

In marine environments, a duct, known as an oceanic evaporation duct, exists up to several meters above the ocean surface. A high refraction index in the duct boundary layer, due to the high humidity at the ocean surface, results in ducting of SHF energy along the surface. The result is that

communication signal propagation ranges are over-the-horizon and extend far beyond expectations. This channel may provide a significant increase in data rate at a range not currently available in present NBG communications.

3.0 SYSTEM DESCRIPTION

This section presents transmitter, receiver, and modem technologies and will be used as a basis for a plausible system description for the analysis of section 5.

3.1 TRANSMITTER

In general, the microwave amplifier, or transmitter, contributes more to the overall performance and system gain than most of the other components composing the transmission system. The microwave power amplifier must deliver a signal of sufficient power to produce an easily detectable output at the end of the transmission channel. This signal should be produced with maximum efficiency, maximum reliability, and minimum distortion.

The characteristics of the microwave power amplifier are identified by the output power level and flatness, the gain, the operating bandwidth, the overall efficiency, the harmonic and intermodulation distortion, the amplitude moduation (AM) to phase modulation (PM) conversion (phase shift of amplified signal), and the noise. To maximize transmission power, yet keep the system complexity at a minimum (i.e., avoid the addition of a water cooling system), a nominal, one-kilowatt microwave transmitter is assumed for the maximum transmission power. Because the system operates at high data rates (using a bandwidth of up to 5 percent of the carrier frequency), the microwave transmitter must operate over large bandwidth excursions. As long as the transmitter can operate in the linear mode, the harmonic and intermodulation distortion can be controlled. However, the efficiency of the microwave amplifier is better (that is, a higher transmitted power is obtained) in the nonlinear region at close to saturation. Unfortunately, the non-linear amplifier causes spectral spreading and increases the AM to PM conversion (increased phase fluctuations) which degrades the system performance.

The microwave devices fall basically into two categories: (1) tubes and (2) semiconductor devices. Figure 3-1 shows the regions where tubes and solid-state devices work best in relation to transmit power and operating frequency. For this particular application using the SHF band, the helix-type traveling wave tube (TWT) meets the requirements. The Helix TWT also provides a large bandwidth excursion which in some cases can be over two octaves (Feher, 1981).

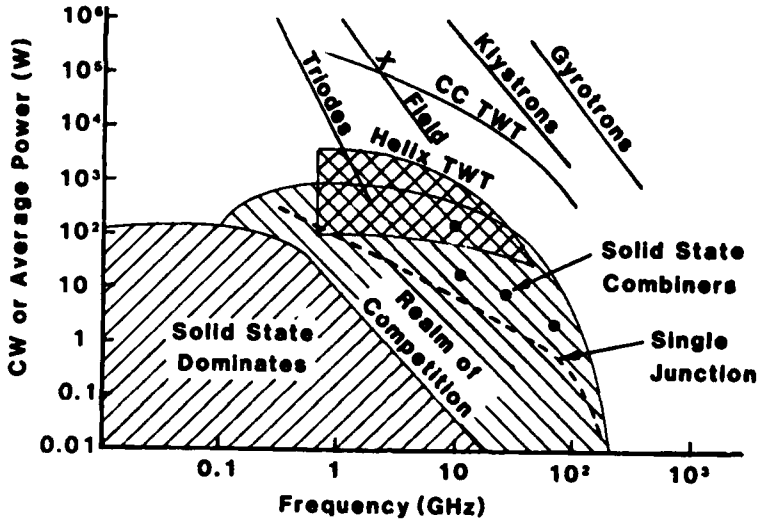

Figure 3-1. Power/frequency relationship of microwave devices.

3.2 RECEIVER

At the reception end of the communication link, the small-signal microwave amplifier must increase the power of a weak signal sufficiently for added processing. In this application, it is critical that the amplifier add as little noise as possible to the signal. Efficiency is usually of secondary concern; the dominate concern is reliability and linearity.

Small-signal amplifiers are evaluated in terms of the following characteristics the gain, the operating bandwidth, and the noise level specified by the noise figure (NF). The third specification is of particular importance. The noise figure (NF), or noise temperature (T_n), describes the deterioration of the signal-to-noise ratio due to the presence of an amplifier. The noise figure is defined as

$$NF(dB) = 10\log_{10}\left[\frac{P_{si}/P_{ni}}{P_{so}/P_{no}}\right], \qquad (3-1)$$

where

P_{si} = available input signal power (watts),

P_{so} = available output signal power (watts),

P_{ni} = available input noise power (watts),

P_{no} = available output noise power (watts).

The output noise power is composed of both the amplified input noise and the inherent amplifier noise P_{inh}. P_{inh} originates in the active and passive elements of the receiver. Mathematically, the output noise power can be expressed as

$$P_{no} = GP_{ni} + P_{inh}, \tag{3-2}$$

where

$$G = \frac{P_{so}}{P_{si}}. \tag{3-3}$$

After combining equations 3-1, 3-2, and 3-3, the noise figure can be written

$$NF(dB) = 10\log_{10}\left[\frac{P_{no}}{GP_{ni}}\right] = 10\log_{10}\left[1+\frac{P_{inh}}{GP_{ni}}\right]. \tag{3-4}$$

The inherent noise of an amplifier is also expressed in terms of its noise temperature T_n which can be represented by

$$P_{inh} = GP_n, \tag{3-5}$$

where P_n is the thermal noise power produced by the matched input load at the temperature T_n such that

$$P_n = kT_nB, \tag{3-6}$$

where

- k = Boltzmann's constant ($1.38 \cdot 10^{-23}$ joules/Kelvin),
- T_n = noise temperature (K), and
- B = amplifier bandwidth (Hz).

Assuming the input noise power P_{ni} of the amplifier is produced by the same matched load at room temperature of $T_0 = 290$ K, the input noise power is

$$P_{ni} = kT_0B. \tag{3-7}$$

The noise figure now becomes

$$NF(dB) = 10\log_{10}\left[1+\frac{T_n}{T_0}\right]. \tag{3-8}$$

Equation 3-8 can also be written as

$$T_n = T_0(10^{NF/10}-1). \tag{3-9}$$

Low-noise gallium arsenide (GaAs) field-effect transistors (FET) have sufficient capabilities to satisfy the requirements in digital communication systems requiring low-noise figures. Typical noise figures at SHF operating frequencies are 5 decibels (dB) or less (Castro and Major, 1988). According to equation 3-9, a noise figure of 5 dB corresponds to a temperature of 627 K.

3.3 MODEM

Because of the importance in transferring information at a high data rate and containing it within a minimal bandwidth, bandwidth-efficient modulation techniques become necessary. Many modulation techniques exist, but QPSK (quaternary phase shift keying) modulation was selected, because it is widely used in many digital terrestrial microwave and satellite systems (Feher, 1981).

Figure 3-2 describes the modulator. The inputs, in-phase (I) and quadrature (Q), represent the sequences of data to be modulated. The digital-to-analog (D/A) converters change the data into analog sequences (a_n) and (b_n), which are then past through a low-pass filter to form the pulse streams $\sum a_n h(t-nT)$, $\sum b_n h(t-nT)$. The low-pass filter has an impulse response h(t) in a raised cosine form to reduce inter-symbol interference (ISI). The local oscillator (LO) produces a sinusoidal carrier at frequency (f_c) and is usually the intermediate frequency (IF) of the radio (although direct modulation at RF may also be used). The local oscillator, along with its quadrature component modulate the I and Q pulse streams respectively. These outputs are added together and then bandpass filtered to produce the signal

$$s(t) = \sum_n a_n h(t-nT)\cos\omega_c t - \sum_n b_n h(t-nT)\sin\omega_c t \qquad (3-16)$$

at the IF or RF (Ivanek, 1989).

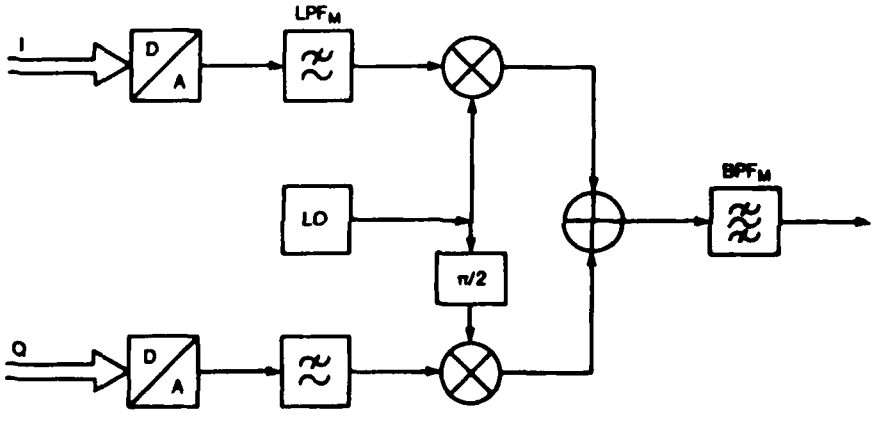

Figure 3-2. QPSK modulator.

Figure 3-3 shows the demodulation process. The incoming modulated signal is passed through a bandpass filter (BPF) to eliminate out-of-band noise and adjacent channel interference. The signal is split into an I and Q demodulation path where the carrier recovery (CR) subsystem regenerates the unmodulated sinusoidal carrier. The reconstituted carrier and its quadrature component are mixed with the I and Q demodulated lines respectively. These lines are low-pass filtered and analog-to-digitally (A/D) converted under the control of the timing recovery (TR) circuitry, to reproduce the I and Q sequences of data that were originally modulated (Ivanek, 1989).

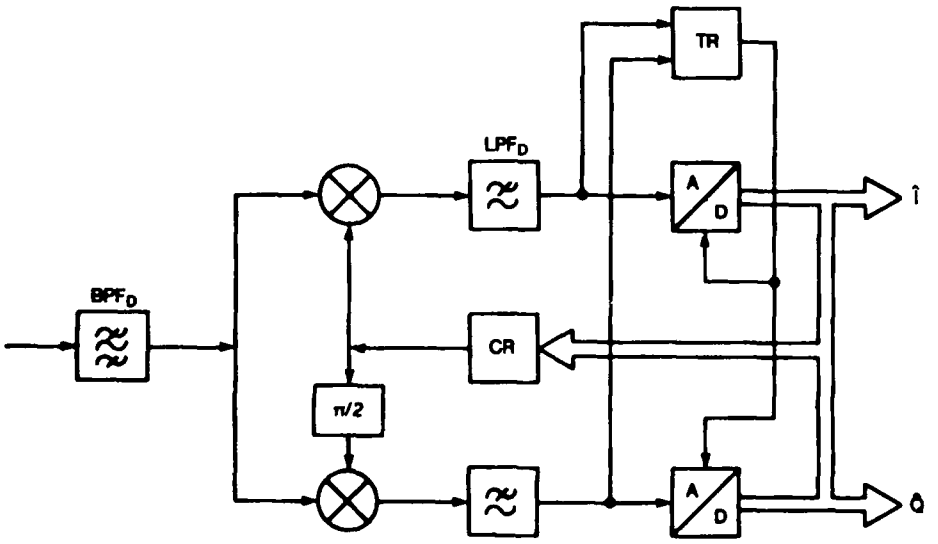

Figure 3.3 QPSK demodulator.

Figure 3-4 depicts the CR subsystem. The carrier recovery is accomplished by passing the IF signal through a nonlinear circuit made up of an *n*th order squarer (i.e. for QPSK, M=4), which removes the modulation from the carrier. The desired spectral component is bandpass filtered. A phase lock loop (PLL) is used to track and produce a clean sinusoidal output which is divided down by *n* to the original modulated frequency. The TR subsystem is accomplished by squaring the output of the low-pass filters, extracting from the square a spectral line component at $1/T$ with the aid of a bandpass filter, and then tracking and cleaning it with a PLL (Ivanek, 1989).

The error performance of this modulator-demodulator (modem) is derived in the following manner. For M-ary PSK system in additive white gaussian noise (AWGN), an ideal, coherent, digital phase detector observes a sinewave with one of M phases. For QPSK, M equals four. For binary phase shift keying (BPSK), M equals two. The detector may be characterized as a device that performs a phase measurement during a T-sec interval. The received wave plus noise is

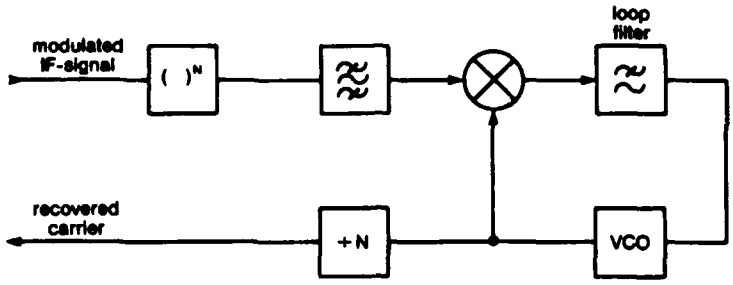

Figure 3-4. QPSK carrier recovery subsystem.

$$r(t) = A\cos(\omega_c t + \phi) + n_c(t)\cos(\omega_c t + \phi) + n_s(t)\sin(\omega_c t + \phi) \qquad (3-17)$$

where $\phi = m(2\pi/M), m = 1, 2, \ldots, M$, and $n_c(t)$ and $n_s(t)$ are the in-phase and quadrature gaussian noise components, respectively, with average power N. Since the transmitted phases are constant over this T-sec interval, the composite phase is

$$\alpha \;=\; \phi + \tan^{-1}\left[\frac{n_s(t)}{A + n_c(t)}\right]. \qquad (3-18)$$

In the absence of noise, the ideal phase detector measures ϕ at the end of the signaling interval. Because of noise, errors are committed whenever the device measures a phase outside of the region

$$\phi - \frac{\pi}{M} \le \theta < \phi + \frac{\pi}{M}. \qquad (3-19)$$

The probability density of the received wave plus noise phase has been derived (Lucky, 1968) and is

$$p(\theta) = \frac{1}{2\pi} e^{-S/N}\left[1 + \sqrt{4\pi S/N}\cos\alpha\, e^{S/N\cos^2\alpha}\, Q(\sqrt{2S/N}\cos\alpha)\right] \qquad (3-20)$$

where

$$Q(x) \;=\; \frac{1}{\sqrt{2\pi}}\int_x^{\infty} e^{-t^2/2}dt \qquad (3-21)$$

and $S/N = A^2/2/N$ is the signal-to-noise ratio.

Assuming all the phase modulations are equally likely, the probability of a phase detected error P_{SE} is given by

$$P_{SE} \;=\; \int_{\pi/M}^{\pi} p(\alpha)\,d\alpha + \int_{-\pi}^{-\pi/M} p(\alpha)\,d\alpha \;=\; 2\int_{\pi/M}^{\pi} p(\alpha)\,d\alpha. \qquad (3-22)$$

For BPSK and QPSK, there exists a closed form solution. These solutions, shown in figure 3-5 are mathematically represented for BPSK as

$$P_{SE}(M=2) = Q(\sqrt{2S/N}) \quad (3-23)$$

and for QPSK as

$$P_{SE}(M=4) = 1-[1-Q(\sqrt{S/N})]^2 \quad (3-24)$$

A listing of the computer code for solving equation 3-23 and 3-24 is given in appendix A.

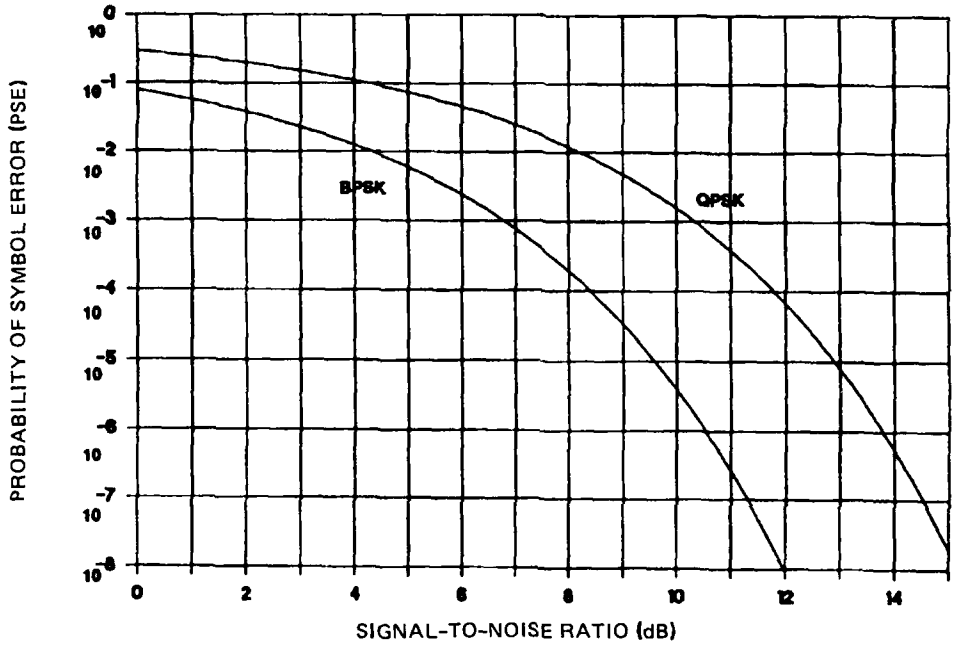

Figure 3-5. BPSK and QPSK probability of symbol error.

For the probability of a bit error P_{BE}, the symbol error rate and bit error rate are related as follows:

$$P_{BE} = \frac{M/2}{M-1} P_{SE}. \quad (3-25)$$

The bit energy E_b to noise power density N_0 is related to the received signal-to-noise ratio by

$$\frac{E_b}{N_0} = \frac{W}{R}\frac{S}{N} = \frac{S/R}{N_0} \quad (3-26)$$

where

$$R = \frac{\log_2 M}{T} \quad (3-27)$$

is the information bit rate (bps), and W is twice the amplifier bandwidth B. Figure 3-6 shows the probability of a bit error, given the energy per bit to noise power density for both BPSK and QPSK. For acceptable digital communications the bit error rate usually ranges from 10^{-3} to 10^{-6}. To be conservative, this system evaluation assumes a bit error rate of 10^{-6} which implies a bit energy to noise power density of 10.5 dB. Since these curves are optimal, theoretical curves for QPSK modulation, a practical receiver E_b/N_0 assumes an operational performance of 14 dB.

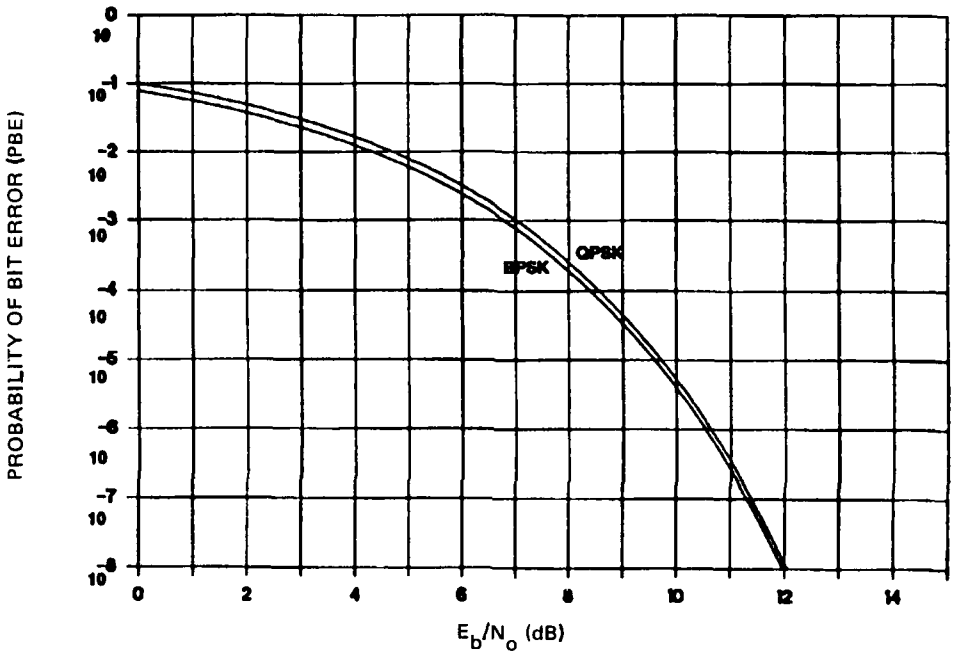

Figure 3-6. BPSK and QPSK probability of bit error.

From the Shannon-Hartley's Theorem, the theoretical efficiency of the channel ζ is related to the signal-to-noise ratio (Bennett & Davey, 1965) by

$$\zeta = \frac{C}{W} = \log_2\left(1+\frac{S}{N}\right) \quad bps/Hz. \qquad (3-28)$$

where C is the channel capacity in bits per second. The channel efficiency for QPSK is related to the signal state and the relation of the low-pass filter in the modem as it compares to the theoretical Nyquist filter characterized by α. The efficiency is expressed (Ivanek, 1989) as

$$\zeta = \frac{R}{W} = \frac{\log_2 M}{(1+\alpha)}. \qquad (3-29)$$

Theoretically, QPSK could have a channel efficiency of 2 bps/Hz (Bennett & Davey, 1965), but since ideal Nyquist sampling filters are not practical ($\alpha = 0$) a more practical filter would have an $\alpha = 0.3$. This implies an efficiency of 1.54 bps/Hz. To be conservative, the efficiency for this problem will assume $\zeta = 1$ bps/Hz.

Considerable attention is now being focused on increasing the information bit throughput rate in a bandlimited channel. For terrestrial microwave link development in the 1980's, the modulation schemes concentrated on quadrature amplitude modulation (QAM) and increasing the signaling space to as high as 1024-ary (Ivanek, 1989). This allows a higher data rate in the same bandwidth, but requires a higher signal-to-noise ratio. If QAM were used for this particular system application, the operation range would be reduced, presuming the same technology, and the advantage given by the evaporation duct would be possibly defeated.

3.4 ANTENNAS

Antennas are described primarily by gain and physical size. Gain and physical size are interdependent. Transmitting and receiving antennas in a microwave system tend to be directive. Thus, the antenna beamwidth (the half-power points) is also of interest. If the required antenna gains are less than 20 dB, a horn antenna is usually used. If an antenna gain over 20 dB is required, a parabolic dish is used (Castro & Major, 1988).

From discussion presented in the following sections, it appears that reasonably sized antennas can be built with gains of approximately 30 dB. The beamwidths are large enough so as not to present difficult pointing problems.

3.4.1 Conical Horn

The horn antenna is a device which effects a transition between wave propagation in a transmission line, usually a waveguide, to waves propagating in free space. The horns are constructed in a variety of shapes to control gain and beamwidth. The types most commonly used are rectangular and conical guides. For a conical or round guide, the optimal gain G in dB and beamwidth BW in degrees are given by the following

$$G = 8.394 + 20\log(D/\lambda) \qquad (3-30)$$

and

$$BW = \frac{58}{(D/\lambda)}. \qquad (3-31)$$

D is the diameter of the circular aperture, and λ is the wavelength (Johnson & Jasik, 1984; Kraus, 1950). The antenna efficiency is assumed to be 70%. The gain and beamwidths for various diameters at 4.5, 9, and 18 GHz are given in table 3-1.

Table 3-1. Gain and beamwidth for a conical horn antenna.

	4.5 GHz		9 GHz		18 GHz	
Diameter (feet)	Gain (dB)	Beam (deg)	Gain (dB)	Beam (deg)	Gain (dB)	Beam (deg)
0.25	9.6	50.7	15.6	25.4	21.6	12.7
0.5	15.6	23.4	21.6	12.7	27.6	6.3
0.75	19.1	16.9	25.1	8.5	31.1	4.2
1.0	21.6	12.7	27.6	6.3	33.6	3.2
1.25	23.5	10.1	29.6	5.1	35.6	2.5
1.5	25.1	8.5	31.1	4.2	37.2	2.1
1.75	26.4	7.2	32.5	3.6	38.5	1.8
2.0	27.6	6.3	33.6	3.2	39.7	1.6
2.25	28.6	5.6	34.7	2.8	40.7	1.4
2.5	29.6	5.1	35.6	2.5	41.6	1.3
2.75	30.4	4.6	36.4	2.3	42.4	1.2
3.0	31.1	4.2	37.2	2.1	43.2	1.1

3.4.2 Square Horn

For a square horn, the equations are

$$G = 9.443 + 20\log(D/\lambda) \qquad (3-32)$$

and

$$BW = \frac{56}{(D/\lambda)}. \qquad (3-33)$$

D is the length of one side of the square, and λ is the wavelength (Johnson & Jasik, 1984; Kraus, 1950). Again, the antenna efficiency is assumed to be 70%. The gain and beamwidths for various lengths at 4.5, 9, and 18 GHz are given in table 3-2.

Table 3.2 Gain and beamwidth for a square horn antenna.

	4.5 GHz		9 GHz		18 GHz	
Length (feet)	Gain (dB)	Beam (deg)	Gain (dB)	Beam (deg)	Gain (dB)	Beam (deg)
0.25	10.6	49.0	16.6	24.5	22.7	12.2
0.5	16.6	24.5	22.7	12.2	29.7	6.12
0.75	20.2	16.3	26.2	8.2	32.2	4.1
1.0	22.7	12.2	28.7	6.1	34.7	3.1
1.25	24.6	9.8	30.6	4.9	36.6	2.4
1.5	26.2	8.2	32.2	4.1	38.2	2.0
1.75	27.5	7.0	33.5	3.5	39.6	1.7
2.0	28.7	6.1	34.7	3.1	40.7	1.5
2.25	29.7	5.4	35.7	2.7	41.7	1.4
2.5	30.6	4.9	36.6	2.4	42.7	1.2
2.75	31.4	4.4	37.4	2.2	43.5	1.1
3.0	32.2	4.1	38.2	2.0	44.2	1.0

3.4.3 Parabolic Antenna (circular aperture)

The geometric properties of a parabola yield an excellent microwave radiator. The plane at which the reflector is cut-off is called the aperture plane. The surface generated by the revolution of parabola around its axis is called a paraboloid. A paraboloid can be used to concentrate the radiation from an antenna located at the focus to form a beam in the same way that a searchlight reflector produces a light beam. A paraboloid converts a spherical wave originating at the focus into a plane wave at the aperture plane.

For a parabolic reflector with a circular aperture, the equations for gain G and beamwidth BW are

$$G = 6.933 + 20\log(D/\lambda) \qquad (3-34)$$

and

$$BW = \frac{58}{(D/\lambda)}. \qquad (3-35)$$

D is the diameter of the circular aperture, and λ is the wavelength (Johnson & Jasik, 1984). An antenna efficiency of 50% is assumed. The gain and beamwidths for various lengths at 4.5, 9, and 18 GHz are given in table 3-3.

Table 3-3. Gain and beamwidth for a parabolic antenna (circular aperture).

	4.5 GHz		9 GHz		18 GHz	
Diameter (feet)	Gain (dB)	Beam (deg)	Gain (dB)	Beam (deg)	Gain (dB)	Beam (deg)
0.25	8.1	50.7	14.1	25.4	20.1	12.7
0.5	14.1	25.4	20.1	12.7	26.2	6.3
0.75	17.6	16.9	23.7	8.5	29.7	4.2
1.0	20.1	12.7	26.2	6.3	32.2	3.2
1.25	22.1	10.1	28.1	5.1	34.1	2.5
1.5	23.7	8.5	29.7	4.2	35.7	2.1
1.75	25.0	7.2	31.0	3.6	37.0	1.8
2.0	26.2	6.3	32.2	3.2	38.2	1.6
2.25	27.2	5.6	33.2	2.8	39.2	1.4
2.5	28.1	5.1	34.1	2.5	40.1	1.3
2.75	28.9	4.6	34.9	2.3	41.0	1.2
3.0	29.7	4.2	35.7	2.1	41.7	1.1

4.0 PROPAGATION CHANNEL

This section discusses both line-of-sight and over-the-horizon propagation, with a consideration of the effects made by diffraction. ducting, and scattering. It concludes with a discussion of fading and attenuation due to the atmosphere and rain.

4.1 LINE-OF-SIGHT

At radio frequencies above 30 MHz, the ionosphere is unable to refract energy, and the ground wave attenuates to negligible amplitude in a very short distance. Propagation is achieved by means of the space wave traveling between the transmitting and receiving antennas. This space wave has two components. The first component is the signal traveling directly from the transmitting to the receiving antenna. The second component reaches the receiving antenna after reflecting from the earth's surface. As these individual signals travel through space, the signals are attenuated by spreading. This spreading is characterized by an inverse square fall-off with range. Within the horizon, coherent interference occurs between the direct and reflected signals. In a marine environment, these multipath effects are the result of interference of the sea reflected path with the direct path. The effects of the rough sea surface on reducing the reflection coefficient is important in determining the total amount of interference between the two paths.

As the distance between transmitting and receiving antennas becomes greater, it is necessary to take into account the curvature of the earth. Because of earth curvature, the effective antennas heights are reduced below the actual antenna heights. In addition, the curvature of the earth causes the ground-reflected signal to be a diverging rather than a plane wave. As a result, the reflected signal at the receiving antenna is weaker that if the reflection were from a flat surface.

4.2 OVER-THE-HORIZON

4.2.1 Diffraction

When the receiving antenna is below the radio horizon, neither the direct nor the ground-reflected signal are received. However, some energy from the transmitter can reach the receiver by diffracting the signal into this shadow zone. The strength of the diffracted field in this shadow zone depends on the roughness of the earth's surface and the wavelength of the signal.

4.2.2 Ducting

The atmosphere through which the signal energy travels influences the propagation to a significant degree. Gas molecules, especially water vapor, cause the air of the troposphere to have a dielectric constant which is greater than one. The refractive index of air varies with height,

generally decreasing as height increases. In accordance with Snell's Law, energy traveling in the atmosphere will bend away from regions of low refractive index and toward regions of high refractive index. Thus the electromagnetic energy will be bent downwards, ducted to receivers at points beyond the line-of-sight.

In a marine environment there are three distinct types of ducts: elevated ducts, surface-based ducts, and evaporation ducts. An elevated duct is created when a trapping layer is sufficiently high that no rays from a source at the surface will be trapped (Hitney et al., 1985). Elevated ducts are most important when addressing airborne systems. A surface-based duct is created by trapping layers that occur up to several hundred meters in height and extend to the surface. These ducts occur with annual frequencies up to 50% in areas such as the eastern Mediterranean and northern Indian Ocean, but occur annually only 8% of the time world-wide with only 1% occurrence in the North Atlantic. Surface-based ducts are responsible for most reports of extremely long over-the-horizon radar detection and communication ranges. The third type of duct, the evaporation duct, is created by the extremely rapid decrease of moisture immediately adjacent to the sea surface. The strength of the evaporation duct is determined by the parameter "duct height" which is a function of sea temperature, air temperature, relative humidity, and wind speed. These ducts vary between 0 and 40 meters. The wordwide average is 13 meters. The evaporation duct acts as a "leaky" waveguide, hence the location of the antenna is not critical.

The Engineer's Refractive Effects Prediction System (EREPS) was developed by the Naval Ocean Systems Center as a collection of individual programs for evaluating the effect of the atmosphere on propagation (Hitney et al., 1985). EREPS, a follow-on to the Integrated Refractive Effects Prediction System (IREPS) (Patterson et al., 1987), consists of three individual programs: PROPR, SDS, and RAYS. PROPR will calculate the path loss for a variety of environmental conditions. SDS displays an annual historical summary of evaporation duct, surface-based duct, and other meteorological parameters for many 10 by 10 degree squares of the earth's surface. SDS is used as the primary source of environmental data for the PROPR program. RAYS is a ray trace program for displaying trajectories of a series of rays for any user-supplied refractive index profile. EREPS serves as the principal means of evaluating propagation for the purpose of this study.

Results from the EREPS program are shown in tables 4-1, 4-2, and 4-3. Propagation loss in dB is tabulated as a function of evaporation duct height, in meters and range, and distance between transmitting and receiving sub-systems, in nautical miles. In tables 4-1, 4-2, and 4-3 the antenna heights are at 100 feet. For a fixed frequency and duct height, there may be an optimum antenna height for maximum transmission nearer the ocean surface. One hundred feet is the recommended height above the design waterline to assure that the ship-to-ship range is achieved for UHF communications (DuBrul & Peters, 1974). Since the default condition for this SHF system is line-of-sight, the 100-foot height is used as the baseline for this study. From the measurements of Richter and Hitney (1988), the optimum location for antennas is high on the ship. Circular polarization and a wind speed of 15 knots are assumed. Tables 4-1, 4-2, and 4-3 separately consider operating frequencies 4.5, 9, and 18 GHz. As stated in section 3.0, the operating frequencies of 4.5, 9, and 18 GHz were chosen for the purposes of this study. Significant extended line-of-sight signal enhancement below 3 GHz is rare. Enhancement at frequencies above 18 GHz begins to be counteracted by sea-surface roughness and atmospheric absorption.

Table 4-1. Propagation loss, dB (4.5 GHz).

	Evaporation Duct Height (m)					
Range (nmi)	0	5	10	13	15	20
20	146	146	146	146	146	146
30	169	162	152	146	146	148
40	190	180	165	156	150	152
50	200	195	178	165	157	155
60	202	201	189	174	163	157
70	205	205	199	183	170	160
80	207	207	205	190	177	161
90	210	210	210	198	183	163
100	212	212	212	204	189	165
150	222	222	222	222	215	174

Table 4-2. Propagation loss, dB (9 GHz).

	Evaporation Duct Height (m)					
Range (nmi)	0	5	10	13	15	20
20	151	151	151	151	151	151
30	179	160	151	155	164	178
40	202	180	153	159	168	190
50	209	197	160	161	169	191
60	212	209	167	163	170	193
70	214	214	175	165	171	194
80	216	216	181	167	172	195
90	219	219	188	168	173	195
100	222	222	195	170	173	195
150	233	232	225	178	175	197

The evaporation duct height is statistical and depends on the geographical area, season, and time of day. Typical values of duct height vary from 0 to 30 meters. Higher duct heights usually occur in the daytime, in the warmer seasons, and in the more equatorial latitudes. The occurrence statistics of the evaporation duct height for different geographical regions can be obtained from the SDS program of EREPS (Hitney et al., 1988). Figure 4-1 displays these different geographic regions, called Marsden squares. The SDS database shows average duct heights vary from around 5 meters

Table 4-3. Propagation loss, dB (18 GHz).

	Evaporation Duct Height (m)					
Range (nmi)	0	5	10	13	15	20
20	157	157	157	157	157	157
30	190	157	177	190	189	189
40	217	173	181	199	201	201
50	222	188	182	200	203	203
60	225	203	183	202	205	205
70	229	217	185	203	207	207
80	233	227	186	204	209	209
90	235	233	187	206	210	210
100	238	238	189	207	211	211
150	251	251	195	213	217	217

in high-latitude areas to around 16 meters in tropical areas, with the worldwide average being 13.1 meters. Table 4-4 provides statistics on duct height occurrences throughout the world. The average is given at the end of the table. The occurrence statistics for selected regions of the Western Hemisphere are given in table 4-5; those for selected regions of the Eastern Hemisphere are displayed in table 4-6. The duct height which occurs at least 75% of the time worldwide is about 8 meters. For the selected Western Hemisphere areas the average duct heights range from 5.3 to 16.5 meters. The 75% occurrence duct height for Hawaii is about 12 meters; for the Gulf of Alaska, about 2 meters; for the Nothwest Pacific, about 2 meters; and for New Guinea, about 12 meters. For the selected areas of the Eastern Hemisphere the average duct heights range from 7.6 meters to 14.4 meters. The 75% occurrence duct height for the Western Atlantic off the East shores of the United States is about 9 meters; for the North Atlantic near Iceland, about 4 meters; for the Atlantic near the equator, about 12 meters; and for the eastern Mediterranean about 8 meters.

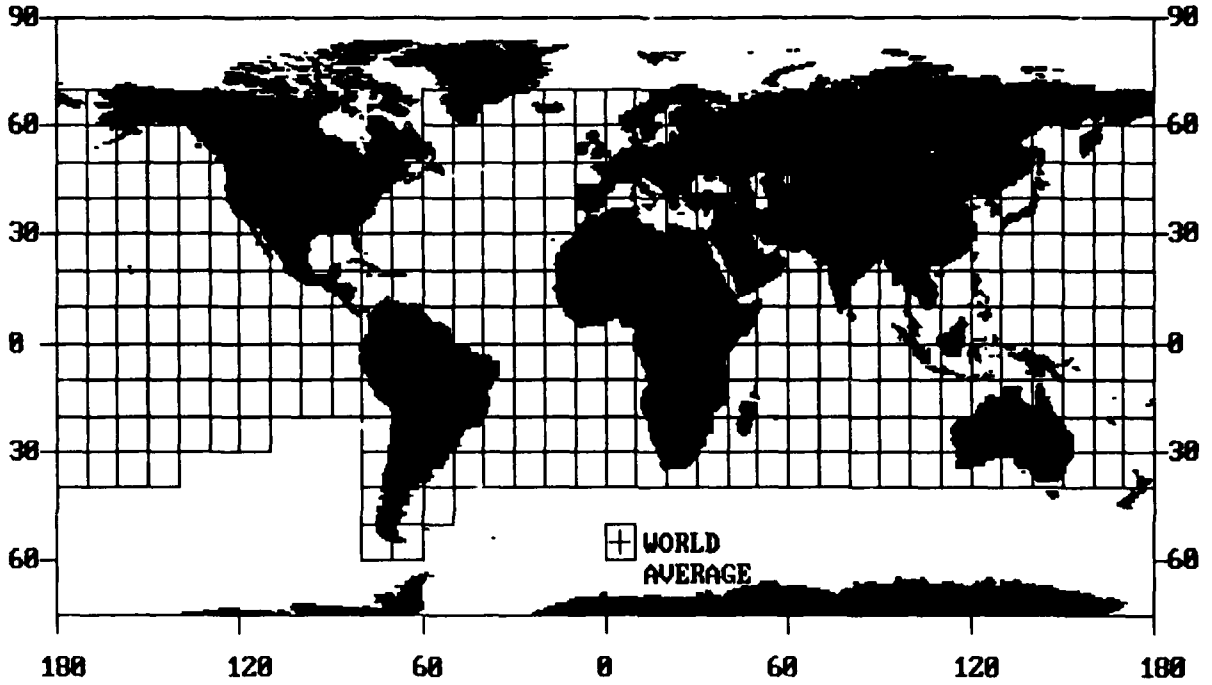

Figure 4-1. Map of Marsden squares.

Table 4-4. Duct height occurrence statistics (worldwide).

Duct Height (meters)	World-wide (%)
0 to 2	5.4
2 to 4	5.0
4 to 6	7.2
6 to 8	8.2
8 to 10	9.2
10 to 12	10.4
12 to 14	10.9
14 to 16	10.5
16 to 18	9.2
18 to 20	7.5
20 to 22	5.8
22 to 24	4.1
24 to 26	2.7
26 to 28	1.7
28 to 30	1.0
30 to 32	0.5
32 to 34	0.3
34 to 36	0.2
36 to 38	0.1
38 to 40	0.0
>40	0.1
AVERAGE (13.1 meters)	

Table 4-5. Duct height occurrence statistics (selected Pacific areas).

Duct Height (meters)	Hawaii (%)	Gulf of Alaska (%)	Northwest Pacific (%)	New Guinea (%)
0 to 2	1.3	20.5	22.2	0.6
2 to 4	1.0	17.7	16.6	0.6
4 to 6	2.4	21.9	18.8	2.6
6 to 8	3.5	17.9	15.2	4.0
8 to 10	5.8	11.7	10.9	6.6
10 to 12	8.7	5.9	7.1	10.6
12 to 14	11.7	2.7	4.3	14.1
14 to 16	13.2	1.1	2.4	14.3
16 to 18	13.2	0.4	1.3	13.2
18 to 20	11.8	0.1	0.7	10.5
20 to 22	9.6	0.1	0.3	8.
22 to 24	6.9		0.1	
24 to 26	4.6		0.1	
26 to 28	2.8			
28 to 30	1.7			
30 to 32	0.9			
32 to 34	0.4			
34 to 36	0.2			
36 to 38	0.1			
38 to 40	0.1			
>40	0.1			
AVERAGE	16.5 m	5.3 m	5.8 m	15.9 m

For this study, the baseline height for the transmitting and receiving antennas is 100 feet. However, for a fixed frequency and duct height, there may be an optimum antenna height for maximum transmission. If economics justify two antennas, an advantage may be obtained with both a high and low antenna. Tables 4-7, 4-8, and 4-9 address antenna heights, using the frequency 9 GHz, and assuming circular polarization. For table 4-7, both the transmitting antenna (Tx) and the receiving antenna (Rx) are at 50 feet. In table 4-8, the transmitting antenna is at 100 feet and

Table 4-6. Duct height occurrence statistics
(selected Atlantic areas).

Duct Height (meters)	Western (USA) (%)	North (Iceland) (%)	Atlantic (Equator) (%)	Eastern (Med) (%)
0 to 2	5.9	12.1	0.7	2.0
2 to 4	2.9	10.6	0.9	3.4
4 to 6	4.8	13.4	2.5	6.7
6 to 8	6.2	16.8	4.1	9.5
8 to 10	7.8	16.7	7.5	11.8
10 to 12	9.5	13.9	10.9	13.4
12 to 14	10.7	8.9	13.1	12.9
14 to 16	10.9	4.7	14.0	11.2
16 to 18	10.5	2.0	13.4	8.7
18 to 20	8.9	0.6	11.3	6.7
20 to 22	7.2	0.2	8.8	4.6
22 to 24	5.3	0.1	6.0	3.2
24 to 26	3.5		3.4	2.1
26 to 28	2.3		1.7	1.4
28 to 30	1.4		1.0	0.9
30 to 32	0.9		0.4	0.5
32 to 34	0.5		0.2	0.4
34 to 36	0.3		0.1	0.2
36 to 38	0.2			0.1
38 to 40	0.1			0.1
>40	0.2			0.2
AVERAGE	14.4 m	7.6 m	15.6 m	13.1 m

the receiving antenna is at 50 feet. In table 4-9, the transmitting antenna is at 50 feet and the receiving antenna is at 100 feet. Those values representing a 4 dB advantage over the baseline case of table 4-2 are highlighted in **bold** and *italics*.

Table 4.7 Propagation loss (50 ft Tx and 50 ft Rx), dB.

	Evaporation Duct Height (m)					
Range (nmi)	0	5	10	13	15	20
20	167	153	151	151	152	167
30	197	174	151	151	***160***	182
40	207	192	155	***154***	***161***	***183***
50	210	205	163	***155***	***162***	***184***
60	213	213	170	***158***	***163***	***185***
70	215	215	176	***159***	***164***	***186***
80	218	218	183	***161***	***165***	***187***
90	221	221	191	***163***	***166***	***188***
100	222	222	197	***165***	***166***	***189***
150	233	233	226	***173***	***167***	***190***

Table 4-8. Propagation loss (100 ft Tx and 50 ft Rx), dB.

	Evaporation Duct Height (m)					
Range (nmi)	0	5	10	13	15	20
20	156	151	151	151	151	156
30	188	166	151	153	163	184
40	203	180	154	156	164	187
50	209	202	161	158	165	188
60	212	210	168	160	166	189
70	215	215	175	162	167	190
80	218	218	182	164	168	191
90	220	220	189	165	169	191
100	222	222	197	168	169	192
150	233	233	225	176	171	194

Table 4-9. Propagation loss (50 ft Tx and 100 ft Rx), dB.

	Evaporation Duct Height (m)					
Range (nmi)	0	5	10	13	15	20
20	156	151	151	151	151	156
30	189	166	151	151	163	184
40	206	186	153	155	165	186
50	209	202	161	158	166	188
60	213	211	169	160	167	189
70	215	215	175	162	167	190
80	217	217	182	163	168	191
90	220	220	189	166	169	191
100	222	222	197	168	169	192
150	233	233	225	175	171	194

Table 4-7 indicates that when both the transmitting and receiving antennas are situated at 50 feet and the evaporation duct height is 13 meters or greater, the propagation loss is up to 8 dB less. Tables 4-8 and 4-9 indicate that transmitting and receiving antennas at different heights provide little advantage.

4.2.3 Scattering

When no ducting occurs, the strength of a microwave signal may be greater than expected on the basis of diffraction. Because of turbulence and other more gradual changes in the troposphere, small irregularities occur in the refractive index (International Telephone and Telegraph Corporation, 1969; Panter, 1972). The signal energy passing through the troposphere will be scattered into the shadow zone. Propagation from a transmitter to a receiver can be achieved using these irregularities in the troposphere. Long distance communication links of several hundred miles can be established using large power and high-gain antennas.

A scattered signal at a particular instant in time appears to be the result of a number of individual signals arriving with random phase differences. Consider the transmitter and receiver antenna beams intersecting on a common volume in the troposphere. Different parts of the scatter volume contribute to the scattered wave. The received signal consists of many components which have traveled slightly different paths. Thus the signal is always varying. Over a period of a few minutes this random variation in signal appears to be Rayleigh distributed. For longer periods the distribution is log normal.

Very narrow beamwidths, diversity techniques (frequency and spatial), and careful selection of modulation techniques are used to overcome the effects of short term fading (Panter, 1972). The long-term signal variations average 10 dB. The summer signal levels average 10 dB higher than in the winter. The atmosphere is well mixed during the afternoon. The signal fade is 5 dB lower than in the morning or evening. Finally, the longer paths exhibit less variability.

Several different approaches exist for the estimation of troposcatter loss; there is no exact method. The loss can be estimated from empirical data. As discussed, the scatter loss is a time-varying quantity. EREPS uses a combination of methods (Panter, 1972). In tables 4-1, 4-2, and 4-3 the propagation due to diffraction and troposcatter is the condition of zero duct height. For the case of zero duct height, the evaporation duct does not exist, and propagation effects are dominated by the diffraction and scattering processes.

4.3 FADING

The atmosphere is an inhomogeneous transmission medium. Variations in the index of refraction are caused by spatial variations in temperature, pressure, humidity, and turbulence. Because of this differential refraction, rays will travel over slightly different path lengths between the transmitter and the receiver. Since the received signal is the vector sum of the rays, the rays can interfere with each other, resulting in a fluctuating (or fading) signal. The resultant multipath propagation can produce a loss that varies with frequency within the radio channel, often called selective fading. The deepest fades tend to be highly selective.

Several quantitative statements can be made from the experimental observations that have been made on fading. First, the cumulative distributions of fading amplitudes are well approximated by 10 dB per decade of probability (Ivanek, 1989). In other words, the amplitude distributions of most deep fades in non-diversity systems vary directly as the square of the reference level. Second, the time during which a received signal is below a certain level is called the "duration of fade." A convenient formula for determining the average duration of a fade T_F in seconds is

$$T_F = 410/10^{F/20} \qquad (4-1)$$

where F is the depth of the fade in decibels (Feher, 1981). A 40-dB fade lasts an average of 4 seconds. It is not obvious that this empirical formula translates to the marine environment and is representative of performance in a ducting channel.

In Richter and Hitney (1988), measurements are given for a 20-nautical mile path in the Southern California off-shore area and for a 14.4-nautical mile path between Key West and the Marquesas Keys. Richter and Hitney (1988) also documents extensive evaporation duct measurements conducted in the eastern Mediterranean, off Greece, for a path 19-nautical miles long. The purpose of the measurements was to provide data for the model validations. These measurements were also used to determine the extent of fading. Fading was defined as the maximum deviation from the mean signal during a 5-minute period. Rapid fluctuations were suppressed by the 4-second time constant in the receiver. A summary profiling the percentage of time a given

fade was exceeded, is presented in tables 4-10 and 4-11. While a number of antennas at different heights and using different operating frequencies were used in the experiments, the results of tables 4-10 and 4-11 were for the highest antenna and 9.624 GHz.

Table 4-10. Percentage of time fade is exceeded (Southern California, Key West).

	Southern California		Key West	
Fade	July	Nov	May	Feb
>20 dB	0	0.2	0	0
>15 dB	0	0.7	0.8	0
>10 dB	0	3.4	2.7	0.1
> 8 dB	0	5	8.5	0.2
> 6 dB	0	6.5	19.4	0.8
> 5 dB	0.1	7.2	23.5	1.1
> 4 dB	0.2	10.2	33.3	3.5
> 3 dB	0.3	16.5	49.8	13.6
> 2 dB	0.9	39.5	83.9	46.8
> 1 dB	4.7	92.7	92.5	87.4

As a rule, the higher fluctuations were observed for weaker signals. At X-band (i.e., 9 to 11 GHz) fading was minimal during the winter in the Mediterranean, exceeding 4 dB only 2% of the time. During the summer, the fading exceeded 15 dB 3% of the time. Interestingly, 10 dB was exceeded on the lower antenna 3% of the time. In the Florida measurements of May the fading exceeded 10 dB 3% of the time. During the Southern California measurements, the fading was minimal. This data was collected at "near" over-the-horizon ranges. Although there is no specific reason to believe that the effects of the duct do not extend further out, there is little data available to prove it.

These single frequency data on fading, although quite extensive, are of limited value for the design of a large bandwidth system susceptible to RF channel distortion. The extent of the multipath fade is frequency dependent. For narrow band FM radio systems where received power at the carrier frequency determines the quality of the digital signal, the statistics of single-frequency fading determines the performance statistics. This relationship may also be true for narrow band or low capacity digital systems. In contrast, a spectrally efficient digital radio signal does not have redundant information in its sidebands. Consequently, the selective loss of some of its frequency components can affect the detectability of the received signal.

Table 4-11. Percentage of time fade is exceeded (Greece).

	Greece		
Fade	Apr	Aug	Nov
>20 dB	0.1	2.2	0
>15 dB	1.7	3.3	0
>10 dB	3.2	9.7	0
> 8 dB	7.2	17.7	0.2
> 6 dB	12.5	33.1	0.5
> 5 dB	14.1	41.4	0.7
> 4 dB	20.2	60.5	2.0
> 3 dB	27.9	78.9	4.6
> 2 dB	41.5	94.3	15.3
> 1 dB	85.2	99.9	39.7

The effect of fading can be minimized with space or frequency diversity techniques, which are based on the hypothesis that simultaneous fading on both radio transmission paths is unlikely. To conserve bandwidth, space diversity is more often used. In the space diversity system the same radio frequency band is used for the transmission of the digital information. Two receiving antennas are vertically separated, which allows the received signal to travel through different transmission paths. Thus the different signals would not likely be affected the same by fading.

During periods of multipath, deep fades on two vertically spaced antennas seldom overlap in time. Thus the cumulative distribution of fading amplitudes will now follow the fourth power of the reference level. The fade duration time, equation 4-1, will be reduced by the following factor

$$F = 2.22x10^{-3} S^2 f/d F^2 \qquad (4-2)$$

where S is the center to center vertical separation of receiving antennas in meters, f is the operating frequency in GHz, and d is the path length in nautical miles. Assuming a spacing of 10 meters between the two diversity antennas, an operating frequency of 9 GHz and a path length of 30 nautical miles, the improvement factor for a fade F of 30 dB is 60. Fading is a concern, and further measurements are required in order to determine the effect of fading on communication performance for this wide-band SHF system concept and the desirability of space diversity.

4.4 ATTENUATION

4.4.1 Atmosphere

Of the gas in the atmosphere, water vapor and oxygen are the principal absorbers of energy from an electromagnetic signal. Water vapor absorbs because of its electric dipole moment. Oxygen absorbs because of its magnetic dipole moment. Oxygen shows maximum absorption around 23 GHz. Water vapor has a maximum at 60 GHz. For these reasons this system application should consider frequencies below 20 GHz. For the purposes of this study frequencies at 4.5, 9, and 18 GHz are considered.

4.4.2 Rain

In addition to clear air atmospheric absorption, rain and fog will also affect absorption. Ice or snow do not produce significant attenuation. Only regions with liquid water precipitation particles are of interest in the estimation of attenuation. Rain attenuation at SHF frequencies can be high. The attenuation per unit distance, A, is the quantity used for calculating rain attenuation. Olsen, Rodgers, and Hodge (1978) developed an empirical procedure based on the approximate relation between A and the rain rate R,

$$A = aR^b \qquad (4-3)$$

where a and b are functions of frequency and rain temperature. This empirical procedure is based on the Laws and Parsons (1943) drop-size distribution, probably the most widely tested distribution. It is a reasonable choice for a mean drop-size spectrum in continental temperate rainfall (Laws & Parsons, 1943; Medhurst, 1965; Ippolito, 1983). In the frequency range between 7 and 32 GHz, the parameter a and, to some extent the parameter b are least sensitive to drop-size distribution.

The loss for different rain rates in dB per nautical mile is given in table 4-12. The effective attenuation losses are again for 4.5, 9, and 18 GHz. The rain rates are in millimeters per hour and are characterized from a drizzle to heavy rain.

Table 4-12. Rain attenuation loss rate, dB/nmi.

Rate (mm/hr)	Rain Type	4.5 GHz	9 GHz	18 GHz
0.25	Drizzle	0.0002	0.0009	0.0052
1.15	Light	0.001	0.0055	0.029
12.5	Medium Heavy	0.013	0.093	0.43
25	Heavy	0.027	0.21	0.93

The Global Prediction Model (Ippolito, 1983) uses cumulative rain rate data to develop statisitcs on total attenuation. This model provides distribution estimates of the instantaneous point rain rate, R, for broad geographical regions. Eight climate regions, A through H, are designated to classify regions covering the entire globe. Figure 4-2 shows the geographical rain climate regions for the continental and ocean areas of the earth. Table 4-13 provides rain rate distribution values (mm/hr) versus percent of the year rain rate is exceeded.

A path-averaged rainfall rate

$$R_{av} = rR \qquad (4-4)$$

where r is defined as the effective path average factor can be used for an estimation of attenuation. The path-averaged rain rate may differ significantly from the surface point rain rate. The estimation of the path-averaged values from the surface point values requires detailed information about the spatial correlation function for rain rate. Adequate spatial data are not currently available. This study assumes that the path average factor r is one.

Using equation 4-3 and the rain rates of table 4-13, the rain attenuation in dB can be computed for different climate regions and ranges. Tables 4-14, 4-15, and 4-16 provide rain attenuation data computed for 4.5, 9, and 18 GHz. The rain attenuation values listed are only exceeded one percent of the year.

It does not appear that rain attenuation is much of a factor at 4.5 GHz (table 4-14). In table 4-15, which profiles figures at 9 GHz, the loss exceeds 3 dB, only in regions E, G, and H. These climate regions are located near the equator. The loss at 18 GHz, exhibited in table 4-16, appears to be almost a factor of 5 greater. From a rain attenuation point of view it would be more desirable to have the lower operating frequencies.

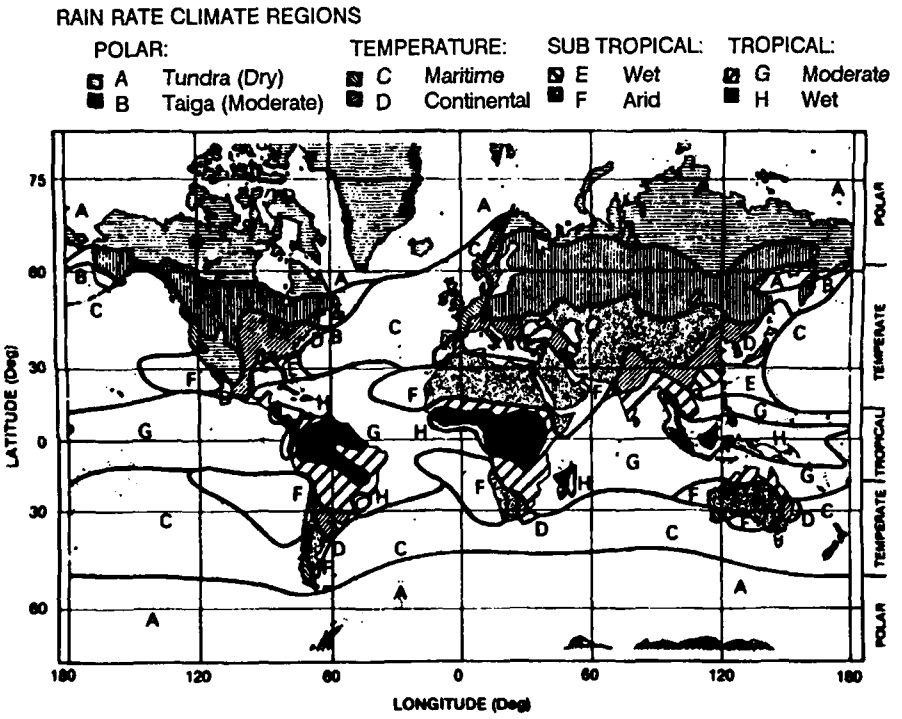

Figure 4-2. Rain climate regions.

Table 4-13. Rain rates - mm/hr.

CLIMATE REGION	PERCENTAGE OF YEAR RAIN RATES ARE EXCEEDED		
	.01%	.1%	1%
A	10	2.5	0.4
B	19.5	5.2	1.3
C	28	7.2	1.8
D	49	14.5	3.0
E	98	35	6.0
F	23	5.2	0.7
G	94	32	8.0
H	147	64	12.0

Table 4-14. Rain attenuation, dB (4.5 GHz) (1% of Year).

CLIMATE REGION	RANGE (nmi)					
	20	40	60	80	100	150
A	0.01	0.01	0.02	0.03	0.03	0.05
B	0.02	0.05	0.07	0.09	0.11	0.17
C	0.03	0.07	0.1	0.13	0.16	0.24
D	0.06	0.11	0.17	0.23	0.28	0.43
E	0.12	0.24	0.36	0.48	0.60	0.90
F	0.01	0.02	0.04	0.05	0.06	0.09
G	0.16	0.33	0.49	0.65	0.82	1.23
H	0 25	0.51	0.76	1.01	1.27	1.90

Table 4-15. Rain attenuation, dB (9 GHz) (1% of Year).

CLIMATE REGION	RANGE (nmi)					
	20	40	60	80	100	150
A	0.03	0.06	0.09	0.12	0.16	0.23
B	0.13	0.25	0.38	0.51	0.63	0.95
C	0.19	0.37	0.56	0.75	0.93	1.40
D	0.34	0.68	1.03	1.37	1.71	2.56
E	0.78	1.56	2.34	3.12	3.89	5.84
F	0.06	0.12	0.18	0.24	0.30	0.45
G	1.10	2.19	3.29	4.39	5.48	8.22
H	1.78	3.55	5.33	7.10	8.88	13.31

Table 4-16. Rain attenuation, dB (18 GHz)
(1% of Year).

CLIMATE REGION	RANGE (nmi)					
	20	40	60	80	100	150
A	0.18	0.35	0.53	0.71	0.88	1.33
B	0.67	1.33	2.00	2.67	3.33	5.00
C	0.96	1.92	2.88	3.84	4.81	7.21
D	1.71	3.42	5.12	6.83	8.54	12.81
E	3.73	7.45	11.18	14.91	18.64	27.96
F	0.33	0.66	1.00	1.33	1.66	2.49
G	5.15	10.31	15.46	20.61	25.77	38.65
H	8.13	16.47	24.4	32.54	40.67	61.0

5.0 LINK PERFORMANCE

This section presents an analytical approach for evaluating the SHF non-satellite channel. In turn, this approach is used as the basis for evaluating the performance of a non-satellite SHF NBG communications link.

5.1 APPROACH

Consider a transmitter that has the capability of transmitting P_t watts of power. In free space at a distance of r meters from the transmitter, the signal power density for an isotropic radiator (i.e., transmits uniformly in all directions) will be

$$P_D = \frac{P_t}{4\pi r^2} \qquad (5-1)$$

For a non-isotropic radiator an antenna gain G_t is used to express the increase of directional power as referenced to the isotropic radiator. The signal power density then becomes

$$P_D = \frac{P_t G_t}{4\pi r^2}. \qquad (5-2)$$

At the receiver an antenna is used to intercept or capture the transmitted power. The net signal power flow into the receiving antenna is

$$S = P_D A_r = \frac{P_t G_t A_r}{4\pi r^2} \qquad (5-3)$$

where A_r is the effective intercept area of the receiver.

The receiver antenna gain is related to the receiver capture area by

$$G_r = \frac{4\pi}{\lambda^2}\varepsilon A, \qquad (5-4)$$

where

A = actual area of the receiving antenna,
ε = antenna efficiency,
$A_r = \varepsilon A$ = effective area of the receiving antenna, and
λ = wavelength.

By rearranging the terms in equation 5-4, the effective area of the receiving antenna is

$$A_r = \varepsilon A = \frac{\lambda^2}{4\pi} G_r. \qquad (5-5)$$

By substituting equation 5-5 into equation 5-3, the received signal power becomes

$$S = \frac{P_t G_t G_r}{(4\pi r/\lambda)^2}. \qquad (5-6)$$

To express equation 5-6 as a function of frequency, the wavelength is converted to frequency using the formula, $\lambda f = c$, where c equals the speed of light. Hence the received power is

$$S = \frac{P_t G_t G_r}{(4\pi r f/c)^2} = P_t G_t G_r \tau. \qquad (5-7)$$

The channel transmission τ is

$$\tau = \frac{1}{(4\pi r f/c)^2}. \qquad (5-8)$$

The channel transmission is expressed as the channel transmission path loss

$$L_{dB} = 10\log\frac{1}{\tau} = 20\log(4\pi r f/c). \qquad (5-9)$$

For a transmission channel other than free space L_{dB} includes the additional effects of the propagation medium (e.g. absorption, diffraction, scattering).

The transmitter can be characterized by its effective isotropic radiated power and is defined as

$$EIRP = P_t G_t. \qquad (5-10)$$

The noise energy density is given by

$$N_0 = kT \qquad (5-11)$$

where

k = Botzmann's constant ($1.38\text{x}10^{-23}$), and
T = system equivalent noise temperature (Kelvin).

The resulting received signal power-to-noise energy density ratio is

$$\frac{S}{N_0} = \frac{P_t G_t G_r \tau}{kT} \qquad (5-12)$$

$$= EIRP \cdot G_r/T \cdot \frac{\tau}{k}. \qquad (5-13)$$

The signal power S can be related to the signal energy per bit E_b by

$$S = E_b R \qquad (5-14)$$

where R is the data rate in bits per second. Using equation 5-14, equation 5-13 can be written

$$\frac{E_b}{N_0} = EIRP \cdot G_r/T \cdot \frac{\tau}{k} \cdot \frac{1}{R}. \qquad (5-14)$$

Equation 5-14 can be expressed as

$$\left(\frac{E_b}{N_0}\right)_{dB} = EIRP_{dB} + (G_r/T)_{dB} - k_{dB} - M_{dB} - L_{dB} - R_{dB} \qquad (5-15)$$

where M is introduced as margin and accounts for miscellaneous loss factors.

5.2 ANALYSIS

Equation 5-15 is used as the basis for evaluating the SHF non-satellite channel. First, as discussed in section 3.3, the required E_b/N_0 is given a value of 14 dB for a requirement of bit error rate (BER) of 10^{-6}. Next $EIRP_{dB}$ can be quantified. Equation 5-10 defines $EIRP_{dB}$. As discussed in section 3.1, one kilowatt would be the upper limit for the transmitted power. From section 3.4, reasonably sized antennas can be built with gains of 30 dB. Thus

$$EIRP_{dB} = 10\log_{10}(1000) + 30. \qquad (5-16)$$

Also, $(G_r/T)_{dB} - k_{dB}$ can be quantified. Again, the receiving antenna can be given a gain of 30 dB. According to section 3.2, a receiver noise temperature of 627 K can be assumed. Thus

$$(G_r/T)_{dB} - k_{dB} = 30\,dB - 10\,[\log_{10}(627) - \log_{10}(1.38x10^{-23})] = 230.6\,dB\,. \qquad (5-17)$$

Finally, a value must be assigned to M_{dB}, the margin in this case, 10 dB. Margin is used to account for system uncertainties including uncertainties in the radiated power, and system equivalent noise temperature. Margin is also used to account for uncertainties in the channel. Included in margin is the effect of rain and fading.

Combining the discussion of these previous paragraphs with equation 5-15 yields

$$14\,dB = 60\,dB + 230.6\,dB - 10\,dB - L_{dB} - R_{dB} \qquad (5-18)$$

Rearranging equation 5-18 yields

$$L_{dB} + R_{dB} = 266.6dB \qquad (5-19)$$

Equation 5-19 can be used for the "classic" trade-off between link capacity (i.e. data rate R_{dB}) and link range (i.e. propagation loss L_{dB}). Using the propagation loss results of tables 4-1 through 4-3, the maximum data rate for a given range and evaporation duct height can be determined. These results are tabulated in table 5-1 for 4.5 GHz, table 5-3 for 9 GHz, and table 5-5 for 18 GHz. As discussed in section 3.3, the bandwidth will be limited to 5% of the carrier frequency. Since the

efficiency is equal to one, the maximum data rate is 225 megabits per second (Mb) for 4.5 GHz, 400 Mb for 9 GHz, and 900 Mb for 18 GHz. It is noted that tables 5-1, 5-3, and 5-5 also contain data rates in kilobits per second (Kb). Those values that are in excess of the maximum data rates are highlighted in **bold** and *italic*. For those combinations of ranges and evaporation duct heights that are limited to the maximum data rate, there will be margins greater than 10 dB. The actual margins for the data rates of table 5-1 are given in table 5-2, for table 5-3 in table 5-4 and for table 5-5 in table 5-6.

Table 5-1. Data rate at 4.5 GHz.

	Evaporation Duct Height (m)					
Range (nmi)	0	5	10	13	15	20
20	***225 Mb***	***225 Mb***	***225 Mb***	***225 Mb***	***225 Mb***	***225 Mb***
30	***225 Mb***	***225 Mb***	***225 Mb***	***225 Mb***	***225 Mb***	***225 Mb***
40	46 Mb	***225 Mb***	***225 Mb***	***225 Mb***	***225 Mb***	***225 Mb***
50	4.6 Mb	14 Mb	***225 Mb***	***225 Mb***	***225 Mb***	***225 Mb***
60	2.8 Mb	2.9 Mb	58 Mb	***225 Mb***	***225 Mb***	***225 Mb***
70	1.4 Mb	1.4 Mb	5.7 Mb	***225 Mb***	***225 Mb***	***225 Mb***
80	912 Kb	912 Kb	1.4 Mb	46 Mb	***225 Mb***	***225 Mb***
90	457 Kb	457 Kb	457 Kb	7.2 Mb	***225 Mb***	***225 Mb***
100	288 Kb	288 Kb	288 Kb	1.8 Mb	58 Mb	***225 Mb***
150	29 Kb	29 Kb	29 Kb	29 Kb	144 Kb	***225 Mb***

Table 5-2. System margin, dB (4.5 GHz).

	Evaporation Duct Height (m)					
Range (nmi)	0	5	10	13	15	20
20	***47***	***47***	***47***	***47***	***47***	***47***
30	***24***	***31***	***41***	***47***	***47***	***45***
40	10	***13***	***28***	***37***	***43***	***41***
50	10	10	***15***	***28***	***36***	***38***
60	10	10	10	***19***	***30***	***36***
70	10	10	10	***11***	***23***	***33***
80	10	10	10	10	***16***	***32***
90	10	10	10	10	***11***	***30***
100	10	10	10	10	10	***28***
150	10	10	10	10	10	***19***

Table 5-3. Data rate at 9 GHz.

Range (nmi)	Evaporation Duct Height (m)					
	0	5	10	13	15	20
20	***450 Mb***	***450 Mb***	***450 Mb***	***450 Mb***	***450 Mb***	***450 Mb***
30	***450 Mb***	***450 Mb***	***450 Mb***	***450 Mb***	***450 Mb***	***450 Mb***
40	2.8 Mb	***450 Mb***	***450 Mb***	***450 Mb***	***450 Mb***	46 Mb
50	575 Kb	9.1 Mb	***450 Mb***	***450 Mb***	***450 Mb***	36 Mb
60	288 Kb	575 Kb	***450 Mb***	***450 Mb***	***450 Mb***	23 Mb
70	182 Kb	182 Kb	***450 Mb***	***450 Mb***	***450 Mb***	18 Mb
80	115 Kb	115 Kb	363 Mb	***450 Mb***	***450 Mb***	15 Mb
90	58 Kb	58 Kb	72 Mb	***450 Mb***	***450 Mb***	15 Mb
100	29 Kb	29 Kb	15 Mb	***450 Mb***	***450 Mb***	15 Mb
150	2.3 Kb	2.9 Kb	15 Kb	***450 Mb***	***450 Mb***	9.1 Mb

Table 5-4. System margin, dB (9 GHz).

Range (nmi)	Evaporation Duct Height (m)					
	0	5	10	13	15	20
20	***39***	***39***	***39***	***39***	***39***	***39***
30	***11***	***11***	***39***	***35***	***26***	***12***
40	10	***11***	***37***	***31***	***22***	10
50	10	10	***30***	***29***	***21***	10
60	10	10	***23***	***27***	***20***	10
70	10	10	***15***	***25***	***19***	10
80	10	10	10	***23***	***18***	10
90	10	10	10	***22***	***17***	10
100	10	10	10	***20***	***17***	10
150	10	10	10	***12***	***15***	10

In the absence of a duct, all three frequencies support maximum data rates to line-of-sight distances. As the frequency is increased the data rate increases, but the system margin decreases. At over-the-horizon distances the lower frequency (4.5 GHz) has the higher data rate.

Table 5-5. Data rate at 18 GHz.

Range (nmi)	Evaporation Duct Height (m)					
	0	5	10	13	15	20
20	***900 Mb***	***900 Mb***	***900 Mb***	***900 Mb***	***900 Mb***	***900 Mb***
30	46 Mb	***900 Mb***	***900 Mb***	46 Mb	58 Mb	58 Mb
40	91 Kb	***900 Mb***	363 Mb	5.8 Mb	3.6 Mb	3.6 Mb
50	29 Kb	72 Mb	288 Mb	4.6 Mb	2.3 Mb	2.3 Mb
60	15 Kb	2.3 Mb	229 Mb	2.9 Mb	1.5 Mb	1.5 Mb
70	5.8 Kb	91 Kb	145 Mb	2.3 Mb	91 Kb	91 Kb
80	2.3 Kb	9.1 Kb	115 Mb	1.8 Mb	58 Kb	58 Kb
90	1.5 Kb	2.3 Kb	91 Mb	1.2 Mb	46 Kb	46 Kb
100	724	724	58 Mb	91 Kb	36 Kb	36 Kb
150	36	36	15 Mb	23 Kb	9 Kb	9 Kb

Table 5-6. System margin, dB (18 GHz).

Range (nmi)	Evaporation Duct Height (m)					
	0	5	10	13	15	20
20	***30***	***30***	***30***	***30***	***30***	***30***
30	10	***30***	***11***	10	10	10
40	10	***14***	10	10	10	10
50	10	10	10	10	10	10
60	10	10	10	10	10	10
70	10	10	10	10	10	10
80	10	10	10	10	10	10
90	10	10	10	10	10	10
100	10	10	10	10	10	10
150	10	10	10	10	10	10

For any combination of desired range and evaporation duct height, the frequency for maximum data rate will vary. From 30 nmi to 50 nmi, the optimal frequency is 9 GHz. The exception is that the 4.5 GHz frequency gives a considerably higher data rate when the evaporation duct height does not exist. At 50 nmi and a duct height of 5 meters, 18 GHz gives the highest data rate. From 60 to 150 nmi and a duct height of 13 meters or greater, 9 GHz gives the highest data rate. At 10 meters duct height 9 GHz again gives the highest data rate, except when the range is 90 nmi or greater, for which 18 GHz gives the highest data rate. For no evaporation duct and 5-meter evaporation duct, the highest data rate occurs at 4.5 GHz.

6.0 CONCLUSIONS

6.1 SUMMARY

Tables 5-1 through 5-6 present a summary of the expected performance of a non-satellite SHF Navy Battle Group communications link. These tables are based on the link performance equation 5-15. Section 3 describes the technologies necessary to the communication link. One kilowatt was selected as an upper limit for the transmitted power and 30 dB antennas were assumed. QPSK modulation was selected, and the energy-per-bit to noise density ratio was determined to be 14 dB for a requirement of a bit error rate of 10^{-6}. A noise figure of 5 dB was used for the receiver. Finally, a 10 dB value was assigned for margin. With these assumptions equation 5-19 was derived. Using the propagation loss results of tables 4-1, 4-2, and 4-3, the maximum data rate for a given range and evaporation duct height could be calculated. The maximum data rate was limited by restricting the bandwidth to 5% of the carrier frequency.

Tables 5-1 through 5-6 examine three frequencies, 4.5, 9, and 18 GHz, to span the SHF band. Significant ducting rarely occurs below 3 GHz. Enhancement at frequencies above 18 GHz begins to be countered by sea-surface roughness and atmospheric absorption. As presented in section 4.3.2, the attenuation due to rain becomes considerable above 10 GHz. In the absence of a duct and in the presence of troposcatter propagation all three frequencies support maximum data rates to line-of-sight distances. As the frequency is increased the data rate increases, but the system margin decreases. At over-the-horizon distances the lower frequency (4.5 GHz) has the higher data rate. If the channel is line-of-sight and troposcatter, it appears that performance is greatest when the frequency is lower in the SHF band.

For any combination of desired range and evaporation duct height, the frequency for maximum data rate will vary. From 30 nmi to 50 nmi, the optimal frequency is 9 GHz. The exception is that the 4.5 GHz frequency gives a considerably higher data rate when the evaporation duct height does not exist. At 50 nmi and a duct height of 5 meters, 18 GHz gives the highest data rate. From 60 to 150 nmi and a duct height of 13 meters or greater, 9 GHz gives the highest data rate.

If the communication system is to make best use of the evaporation duct, an operating frequency around 9 GHz appears to be the best choice. However, at this frequency consideration should to be given to the use of diversity.

6.2 RECOMMENDATIONS

The results of this study indicate link performance of potentially great value to the Navy. It is recommended that a program be started to consider the value of a system based on the link. Four principal program efforts are required for the development of a non-satellite NBG communication system. These efforts include system engineering, RF engineering, network engineering, and experimental evaluation. The system engineering effort determines the requirements for the communication system and provides the evaluation of system cost and system performance. System engineering determines the "return on investment" and provides the forum for iteration of

requirements, design, and experiments. RF engineering determines the RF design to meet the requirements and the cost associated with the design. Network engineering determines the network design with the RF design for again meeting the requirements. Experimental evaluation is needed to bound anomalies in the system and propagation channel.

6.2.1 System Engineering

The system engineering effort should work closely with the Warfare System Architecture and Engineering (WSA&E) to define requirements and assess performance. Each of the capabilities and limitations discovered by the engineering efforts will be interrelated. In examining this postulated system concept, a whole host of questions arise in terms of implementation and realization. These are issues to be resolved through the union of cooperative efforts in system engineering, RF design, networking, and experimentation.

6.2.2 RF Design

The RF Design effort would examine the equipment configurations suitable for implementing the system. The transmitter, receiver, and antenna combinations would be examined, and the number of links and their configuration would be investigated in order to establish a reliable relay capability.

6.2.3 Network Design

The network design would model and evaluate the composite of links characterizing the net, and evaluate the merits of proposed system concepts. This paper has examined the feasibility of using a portion of the SHF band, to communicate line-of-sight and beyond, by the existence of an evaporation duct. Coupled to this is the ability of the SHF band to provide the capability of transferring information at extremely high data rates (100's of Mbps). Given these capabilities at extended line-of-sight ranges, what makes sense in terms of a reasonable network configuration?

Within a Navy task force there is a collection of ships which have requirements to exchange several types of information. A network could be established to provide an orderly and time efficient exchange of this information. Using the capabilities offered by this extended line-of-sight, high data rate pipe, a collection of these links could be configured amongst the task force ships to provide information exchange. The analogy is like taking the telephone company to sea where the terrestrial microwave links are now continuously moving.

The types of information to be transferred would comprise data, voice, and video. Each ship would act as a node where information would be received and transmitted. The information collected by the receiver would either be relayed to another node and/or extracted by the receiving node. The node or ship would also have the ability to inject new information into the system. An automated network manager would be developed to insure the most efficient utilization of the assets.

6.2.4 Experimental Evaluation

The great majority of the experimental data collected in investigating the evaporation duct have been collected at "near" over-the-horizon ranges. Although there is no specific reason to believe that the effects of the duct do not extend further out, there is little data available to prove it.

7.0 REFERENCES

Bennett, W. R., and J. R. Davey. 1965. *Data Transmission*, McGraw-Hill Book Company, New York.

Castro, C. R., and R. Major. 1988. "Improved USMC Antenna Farm Downlink," NOSC TN 1557 (November). Naval Ocean Systems Center, San Diego, CA. *

Clapp, G. 1988. "The Impact of Communications on C3I Technology Investment in the 21st Century Navy," *Proceedings of MILCOM 1989*, San Diego, CA., October.

DuBrul, D. W., and L. M. Peters. 1974. "Shipboard Antenna and Topside Arragement Guidance," NELC TD 356 (September). Naval Electronics Laboratory Center, San Diego, CA.

Feher, K. 1981. *Digital Communications: Microwave Applications*, Prentice-Hall, Englewood Cliffs, New Jersey.

Hitney, H. V., J. H. Richter, R. A. Pappert, K. D. Anderson, and G. B. Baumgartner, Jr. 1985. "Tropospheric Radio Propagation Assessment," *Proceedings of the IEEE*, vol. 73(2), February.

International Telephone and Telegraph Corporation. 1969. *Reference Data for Radio Engineers: Fifth Edition*, Howard W. Sams & Co., Inc., New York.

Ippolito, L. 1983. "Propagation Effects Handbook for Satellite Systems Design: A Summary of Propagation Impairments on 10 to 100 GHz Satellite Links with Techniques for System Design." NASA Reference Publication (PR) 1082(03). National Aeronautics and Space Administration, Washington, D.C.

Ivanek, F. 1989. *Terrestrial Digital Microwave Communications*, Artech House, Inc., Norwood, MA.

Johnson, R. C. and H. Jasik. 1984. *Antenna Engineering Handbook - Second Edition*, McGraw-Hill Book Company, New York.

Kraus, J. D., 1950. *Antennas*, McGraw-Hill Book Company, Inc., New York.

Laws, J. O and D. A. Parsons. 1943. "The Relation of Raindrop-size to Intensity," *Transactions of American Geophysical Union*, vol. 24, pp 452-460.

Lucky, R. W., J. Salz, and E. J. Weldon, Jr. 1968. *Principles of Data Communication*, McGraw-Hill Book Company, New York.

Medhurst, R. G. 1965. "Rainfall Attenuation of Centimeter Waves: Comparison of Theory and Measurement," *IEEE Transactions on Antennas and Propagation, AP-13*, July.

Olsen, R. L., D. V. Rodgers, and D. B. Hodge. 1978. "The aR^b Relation in the Calculation of Rain Attenuation," *IEEE Transactions on Antennas and Propagation, AP-26*, March.

* NOSC Technical Notes are working documents and do not represent an official policy statement of the Naval Ocean Systems Center. For further information, contact the author.

Panter, P. F. 1972. *Communication System Design: Line-of-sight and Tropo-scatter Systems*, McGraw-Hill Book Company, New York.

Patterson, W. L., C. P. Hatton, H. V. Hitney, R. A. Paulus, K. D. Anderson, and G .E. Lindem. 1987. "IREPS 3.0 User's Manual," NOSC TD 1151 (September). Naval Ocean Systems Center, San Diego, CA.

Richter, J. H., and H. V. Hitney. 1988. "Antenna Heights for the Optimum Utilization of the Oceanic Evaporation Duct. Part I: Results from the Pacific Measurements, Part II: Results from Key West Measurements, Part III: Results from the Mediterranean Measurements," NOSC TD 1209 vols. 1,2 (January). Naval Ocean Systems Center, San Diego, CA.

APPENDIX A: Computer Code Listing

This appendix lists the equations and the FORTRAN computer code used to generate the performance curves for ideal biphase shift keying (BPSK) and quaternary phase shift keying (QPSK). A closed form solution exists for the performance of ideal BPSK and QPSK modulation. The equation characterizing BPSK is

$$P_{SE}(M=2) = Q(\sqrt{2S/N}) = \frac{1}{2}erfc(\sqrt{S/N}) \qquad (A-1)$$

and the equation characterizing QPSK is

$$P_{SE}(M=4) = 1-(1-Q(\sqrt{S/N}))^2 = 1-\left(1-\frac{1}{2}erfc(\sqrt{S/N/2})\right)^2 \qquad (A-2)$$

where

$$Q(x) = \frac{1}{\sqrt{2\pi}}\int_x^\infty e^{-t^2/2}\,dt, \qquad (A-3)$$

$$erfc(z) = \frac{2}{\sqrt{\pi}}\int_z^\infty e^{-t^2}\,dt, \qquad (A-4)$$

and

$$Q(x) = \frac{1}{2}erfc(x/\sqrt{2}). \qquad (A-5)$$

The FORTRAN computer code listing for equation A-1 and equation A-2 is presented as follows:

```
      implicit real (a-z)
      integer i
      do 10 i=0,150
      snrdb=float(i)/10.
      snr=10.**(snrdb/10.)
      Ps_BPSK=0.5*erfc(sqrt(SNR))
      Ps_QPSK=1.-(1.-0.5*erfc(sqrt(SNR/2.)))**2.
      write(6,*) SNRDB,log10(Ps_BPSK),log10(Ps_QPSK)
10    continue
      end
      REAL FUNCTION ERF(X)
C  ************************************************************
C     FUNCTION RETURNS THE ERROR FUNCTION.  ADAPTED FROM      *
C     MILLER, "PASCAL PROGRAMS FOR SCIENTISTS AND ENGINEERS". *
C     12TH-ORDER POLYNOMIAL FIT FOR ERROR FUNCTION.           *
C  ************************************************************************
C     PROGRAM INPUTS:
C      NAME          TYPE  DESCRIPTION                              UNITS
C      ------------------------------------------------------------------
C       X            REAL  INPUT VALUE                               -
C
C    PROGRAM OUTPUTS:
C      NAME          TYPE  DESCRIPTION                              UNITS
C      ------------------------------------------------------------------
C       ERF          REAL  ERROR FUNCTION                            -
```

```
C
C    SUBROUTINES AND FUNCTIONS CALLED:
C      ERFC
C
C    PROGRAM INTERNAL VARIABLES:
C      NAME          TYPE  DESCRIPTION                                  UNITS
C      ------------------------------------------------------------------------
C      SQRTPI        REAL  SQUARE ROOT OF PI                             -
C      T2..T12       REAL  CURVE FIT PARAMETERS                          -
C  ************************************************************************
      IMPLICIT REAL(A-Z)
      LOGICAL SGN
      PARAMETER (T2=0.6666667,T3=0.2666667
     $          ,T4=0.07619048,T5=0.01693122,T6=3.078403E-3
     $          ,T7=4.736005E-4,T8=6.314673E-5,T9=7.429027E-6
     $          ,T10=7.820028E-7,T11=7.447646E-8,T12=6.476214E-9)
      SQRTPI=SQRT(2.*ACOS(0.))
      Y=X
      SGN=Y.LT.0.
      IF(SGN) Y=ABS(Y)
          IF(Y.GT.1.5) THEN
            TEMP=1.-ERFC(Y)
          ELSE
              IF(Y.EQ.0) THEN
                TEMP=0.
              ELSE
                X2=Y**2
                SUM=T5+X2*(T6+X2*(T7+X2*(T8+X2*(T9+X2*(T10+X2*
     $               (T11+X2*T12))))))
                TEMP=2.0*EXP(-X2)/SQRTPI*(Y*(1.+X2*(T2+X2*
     $                (T3+X2*(T4+X2*SUM)))))
              ENDIF
          ENDIF
      IF(SGN) TEMP=-TEMP
      ERF=TEMP
      RETURN
      END

      REAL FUNCTION ERFC(X)
C  ************************************************************
C     FUNCTION RETURNS THE COMPLIMENTARY ERROR FUNCTION:       *
C     ADAPTED FROM MILLER, "PASCAL PROGRAMS FOR SCIENTISTS AND *
C     ENGINEERS".                                              *
C  ************************************************************************
C     PROGRAM INPUTS:
C      NAME          TYPE  DESCRIPTION                                  UNITS
C      ------------------------------------------------------------------------
C       X            REAL  INPUT VALUE                                   -
C
C    PROGRAM OUTPUTS:
C      NAME          TYPE  DESCRIPTION                                  UNITS
C      ------------------------------------------------------------------------
C       ERFC         REAL  COMPLIMENTARY ERROR FUNCTION                  -
C
C    SUBROUTINES AND FUNCTIONS CALLED:
C     ERF
C     EXP
C
C    PROGRAM INTERNAL VARIABLES:
C      NAME          TYPE  DESCRIPTION                                  UNITS
C      ------------------------------------------------------------------------
C       SQRTPI       REAL  SQUARE ROOT OF PI                             -
C  ************************************************************************
      IMPLICIT REAL(A-Z)
C INITIALIZATION OF VARIABLES
       SQRTPI=SQRT(2.*ACOS(0.))
```

```
      IF(X.LE.1.5) THEN
        ERFC=1.-ERF(X)
      ELSE
        X2=X**2
        V=0.5/X2
        SUM=V/(1.+8.*V/(1.+9.*V/(1.+10.*V/(1.+11.*V/(1.+12.*V)))))
        SUM=V/(1.+3.*V/(1.+4.*V/(1.+5.*V/(1.+6.*V/(1.+7.*SUM)))))
        ERFC=1./(EXP(X2)*X*SQRTPI*(1.+V/(1.+2.*SUM)))
      ENDIF
    RETURN
    END
```

Equations A-6 and equation A-7 are used to convert the symbol error rate into bit error rate, and to convert signal-to-noise ratio into bit energy over noise-power density. These equations are shown below:

$$P_{BE} = \frac{M/2}{M-1} P_{SE}, \qquad (A-6)$$

$$\frac{E_b}{N_0} = \frac{TW}{\log_2 M} \frac{S}{N}. \qquad (A-7)$$

After substitution of equation A-6 and equation A-7 into equation A-1 and equation A-2, a new set of performance equations are produced

$$P_{BE}(M=2) = Q(\sqrt{2E_b/N_0}) = \frac{1}{2} erfc(\sqrt{E_b/N_0}), \qquad (A-8)$$

$$P_{BE}(M=4) = \frac{2}{3}\left(1-(1-Q(\sqrt{2E_b/N_0}))^2\right) = \frac{2}{3}\left(1-\left(1-\frac{1}{2}erfc(\sqrt{E_b/N_0/2})\right)^2\right). \qquad (A-9)$$

The FORTRAN computer code listing for equation A-8 and equation A-9 is presented as follows:

```
      implicit real (a-z)
      integer i
      do 10 i=0,150
      Eb_NodB=float(i)/10.
      Eb_No=10.**(Eb_NodB/10.)
      Pb_BPSK=0.5*erfc(sqrt(Eb_No))
      Pb_QPSK=2./3.*(1.-(1.-0.5*erfc(sqrt(Eb_No)))**2.)
      write(6,*) Eb_NodB,log10(Pb_BPSK),log10(Pb_QPSK)
10    continue
      end
      REAL FUNCTION ERF(X)
C  ****************************************************************
C     FUNCTION RETURNS THE ERROR FUNCTION.  ADAPTED FROM      *
C     MILLER, "PASCAL PROGRAMS FOR SCIENTISTS AND ENGINEERS". *
C     12TH-ORDER POLYNOMIAL FIT FOR ERROR FUNCTION.           *
C  ****************************************************************************
C     PROGRAM INPUTS:
C      NAME          TYPE  DESCRIPTION                              UNITS
C      ------------------------------------------------------------------------
C       X            REAL  INPUT VALUE                               -
C
C    PROGRAM OUTPUTS:
C      NAME          TYPE  DESCRIPTION                              UNITS
C      ------------------------------------------------------------------------
C       ERF          REAL  ERROR FUNCTION                            -
C
C    SUBROUTINES AND FUNCTIONS CALLED:
```

```
C      ERFC
C
C    PROGRAM INTERNAL VARIABLES:
C      NAME          TYPE  DESCRIPTION                                  UNITS
C      ------------------------------------------------------------------------
C      SQRTPI        REAL  SQUARE ROOT OF PI                             -
C      T2..T12       REAL  CURVE FIT PARAMETERS                          -
C  ************************************************************************
      IMPLICIT REAL(A-Z)
      LOGICAL SGN
      PARAMETER (T2=0.6666667,T3=0.2666667
     $          ,T4=0.07619048,T5=0.01693122,T6=3.078403E-3
     $          ,T7=4.736005E-4,T8=6.314673E-5,T9=7.429027E-6
     $          ,T10=7.820028E-7,T11=7.447646E-8,T12=6.476214E-9)
      SQRTPI=SQRT(2.*ACOS(0.))
      Y=X
      SGN=Y.LT.0.
      IF(SGN) Y=ABS(Y)
          IF(Y.GT.1.5) THEN
            TEMP=1.-ERFC(Y)
          ELSE
              IF(Y.EQ.0) THEN
                TEMP=0.
              ELSE
                X2=Y**2
                SUM=T5+X2*(T6+X2*(T7+X2*(T8+X2*(T9+X2*(T10+X2*
     $               (T11+X2*T12))))))
                TEMP=2.0*EXP(-X2)/SQRTPI*(Y*(1.+X2*(T2+X2*
     $                (T3+X2*(T4+X2*SUM)))))
              ENDIF
          ENDIF
      IF(SGN) TEMP=-TEMP
      ERF=TEMP
      RETURN
      END

      REAL FUNCTION ERFC(X)
C  ***************************************************************
C     FUNCTION RETURNS THE COMPLIMENTARY ERROR FUNCTION:       *
C     ADAPTED FROM MILLER, "PASCAL PROGRAMS FOR SCIENTISTS AND *
C     ENGINEERS".                                              *
C  ************************************************************************
C     PROGRAM INPUTS:
C      NAME          TYPE  DESCRIPTION                                  UNITS
C      ------------------------------------------------------------------------
C       X            REAL  INPUT VALUE                                   -
C
C    PROGRAM OUTPUTS:
C      NAME          TYPE  DESCRIPTION                                  UNITS
C      ------------------------------------------------------------------------
C       ERFC         REAL  COMPLIMENTARY ERROR FUNCTION                  -
C
C    SUBROUTINES AND FUNCTIONS CALLED:
C     ERF
C     EXP
C
C    PROGRAM INTERNAL VARIABLES:
C      NAME          TYPE  DESCRIPTION                                  UNITS
C      ------------------------------------------------------------------------
C       SQRTPI       REAL  SQUARE ROOT OF PI                             -
C  ************************************************************************
      IMPLICIT REAL(A-Z)
C INITIALIZATION OF VARIABLES
        SQRTPI=SQRT(2.*ACOS(0.))
        IF(X.LE.1.5) THEN
          ERFC=1.-ERF(X)
```

```
      ELSE
        X2=X**2
        V=0.5/X2
        SUM=V/(1.+8.*V/(1.+9.*V/(1.+10.*V/(1.+11.*V/(1.+12.*V)))))
        SUM=V/(1.+3.*V/(1.+4.*V/(1.+5.*V/(1.+6.*V/(1.+7.*SUM)))))
        ERFC=1./(EXP(X2)*X*SQRTPI*(1.+V/(1.+2.*SUM)))
      ENDIF
    RETURN
    END
```

REPORT DOCUMENTATION PAGE

Form Approved
OMB No. 0704-0188

1. AGENCY USE ONLY *(Leave blank)*	2. REPORT DATE	3. REPORT TYPE AND DATES COVERED
	March 1991	Final: 1 Sep 89 – 31 Dec 89

4. TITLE AND SUBTITLE

BATTLE GROUP ALTERNATIVE COMMUNICATIONS:
A Study of the SHF Non-Satellite Communications Channel

5. FUNDING NUMBERS

Program Element #: 0602232N
Task No.: R3211
Agency Accession #: DN300067

6. AUTHOR(S)

J. W. Rockway and R. R. James

7. PERFORMING ORGANIZATION NAME(S) AND ADDRESS(ES)

Naval Ocean Systems Center
San Diego, CA 92152–5000

8. PERFORMING ORGANIZATION REPORT NUMBER

NOSC TR 1406

9. SPONSORING/MONITORING AGENCY NAME(S) AND ADDRESS(ES)

Office of Chief of Naval Research
Arlington, VA 20217

10. SPONSORING/MONITORING AGENCY REPORT NUMBER

11. SUPPLEMENTARY NOTES

12a. DISTRIBUTION/AVAILABILITY STATEMENT

Approved for public release; distribution is unlimited.

12b. DISTRIBUTION CODE

13. ABSTRACT *(Maximum 200 words)*

While lack of channel and bandwidth availability is the most frequently expressed communications problem in Navy Battle Group (NBG) communications, there is a group of communication channels which is not currently being exploited. This study considers the use of troposcatter and ducting in the Super High Frequency (SHF) band for ship-to-ship communications. Both line-of-sight and over-the-horizon communications are evaluated.

The results of this study indicate link performance of great value to the Navy. A program is recommended to evaluate such a link and to determine the utility for an NBG communications system.

14. SUBJECT TERMS

ship-to-ship communications links
evaporation duct
troposcatter
Engineer's Refractive Effects Prediction System (EREPS)
Super High Frequency (SHF) communications

15. NUMBER OF PAGES

61

16. PRICE CODE

17. SECURITY CLASSIFICATION OF REPORT	18. SECURITY CLASSIFICATION OF THIS PAGE	19. SECURITY CLASSIFICATION OF ABSTRACT	20. LIMITATION OF ABSTRACT
UNCLASSIFIED	UNCLASSIFIED	UNCLASSIFIED	SAME AS REPORT

21a. NAME OF RESPONSIBLE INDIVIDUAL	21b. TELEPHONE *(Include Area Code)*	21c. OFFICE SYMBOL
J. W. Rockway and R. R. James	(619) 553-5688/553-6131	Code 805/844

INITIAL DISTRIBUTION

Code 0012	Patent Counsel	(1)
Code 0144	R. November	(1)
Code 171	A. E. Chagnon	(1)
Code 171	M. B. Vineberg	(1)
Code 543	H. V. Hitney	(1)
Code 543	K. D. Anderson	(1)
Code 543	T. Rodgers	(1)
Code 7602	L. E. Hoff	(1)
Code 805	J. W. Rockway	(10)
Code 808	R. D. Peterson	(1)
Code 808	G. A. Clapp	(1)
Code 824	H. W. Guyader	(1)
Code 824	C. S. Fuzak	(1)
Code 824	J. Rahilly	(10)
Code 844	R. R. James	(10)
Code 844	R. J. Nies	(1)
Code 854	R. L. Merk	(1)
Code 856	C. R. Castro	(1)

Defense Technical Information Center
Alexandria, VA 22304-6145 (4)

NOSC Liaison Office
Washington, DC 20363-5100 (1)

Center for Naval Analyses
Alexandria, VA 22302-0268 (1)

Office of Naval Technology
Arlington, VA 22217-5000 (1)